Journal of Power Sources 185 (2008) 664–669

Contents lists available at ScienceDirect

Journal of Power Sources

journal homepage: www.elsevier.com/locate/jpowsour

Novel Nafion composite membranes with mesoporous silica nanospheres as inorganic fillers

Yonggang Jin[a], Shizhang Qiao[a,*], Lei Zhang[a,b], Zhi Ping Xu[a], Simon Smart[a], João C. Diniz da Costa[a], Gao Qing Lu[a,*]

[a] ARC Centre of Excellence for Functional Nanomaterials, School of Engineering and Australian Institute for Bioengineering and Nanotechnology, The University of Queensland, QLD 4072, Australia
[b] College of Chemistry and Chemical Engineering, China University of Petroleum, Dongying 257061, China

ARTICLE INFO

Article history:
Received 19 May 2008
Received in revised form 18 July 2008
Accepted 22 August 2008
Available online 9 September 2008

Keywords:
Nafion
Mesoporous silica
Nanospheres
Composite membrane
Proton conduction
Proton exchange membrane fuel cell

ABSTRACT

Novel Nafion composite proton exchange membranes are prepared using mesoporous MCM-41 silica nanospheres as inorganic fillers. The novelty of this study lies in the structural design of inorganic silica fillers: the nanosized and monodisperse spherical morphology of fillers facilitates the preparation of homogenous composite membranes, whilst the superior water adsorption of the mesostructure in fillers consigns enhanced water retention properties to the polymer membranes. Scanning electron microscopy images of the composite membranes indicate that well-dispersed silica nanospheres are embedded in the Nafion matrix, but a large amount of added fillers (3 wt.%) causes some agglomeration of the nanospheres. Compared with the Nafion cast membrane, the composite membranes offer improved thermal stability, enhanced water retention properties, and reduced methanol crossover. Despite the enhancement of water retention, the composite membranes still exhibit a proton conductivity reduction of 10–40% compared with pristine Nafion. This is likely due to the incorporation of much less conductive silica fillers than Nafion. The composite membrane containing 1 wt.% of fillers displays the best cell performance in direct methanol fuel cell tests; it gives a maximum power density of 21.8 mW cm^{-2}, i.e., ~20% higher than the Nafion cast membrane. This is attributed to its similar conductivity to Nafion, and its markedly reduced methanol crossover, namely, ~1.2 times lower.

1. Introduction

Proton exchange membrane fuel cells (PEMFCs) are being developed as promising energy delivery devices for applications from vehicles to off-grid power supply and portable electronic devices [1–3]. The solid proton exchange membrane (PEM) is the heart of a PEMFC and functions as the proton conducting electrolyte as well as the gas and electronic separator [4]. For many years, commercial perfluorosulfonic acid (PFSA) polymer membranes such as Nafion from DuPont have been dominant in PEMFCs. They have attractive properties that include good mechanical properties, excellent chemical stability and relatively high proton conductivity at low temperatures (<100 °C) and under high humidity conditions [5–7]. Nevertheless, their inherent drawbacks cannot satisfy the requirements for the latest development of the PEMFC technology. The major challenge to state-of-the-art PFSA membranes is their inability to operate at intermediate temperatures (100–200 °C) due to their glass transition temperature limit and their reliance on water for proton conduction [8]. Increasing the operating temperature of PEMFCs to over 100 °C promises important benefits with respect to the complexity, cost and performance of the fuel cell system [8–10]. The high methanol permeability of PFSA membranes substantially reduces the efficiency of direct methanol fuel cells (DMFCs) as methanol reacts with oxygen at the cathode and thereby gives rise to a mixed potential [11].

To overcome these shortcomings in the properties of PFSA membranes, significant efforts have been made to increase the operating temperature and reduce the methanol permeability through modifying the membranes. Among various methods, an effective way is to recast PFSA-based organic–inorganic composite membranes with hygroscopic inorganic oxide fillers such as silica, titania, zeolite and montmorillonite [12–15]. Inclusion of these inorganic materials primarily improves the thermal stability and water retention properties of PFSA membranes at elevated temperatures. Simultaneously, the composite membranes are generally found to possess reduced methanol permeability due to depressed methanol crossover caused by introducing inorganic materials in the flow channels [16]. Moreover, bifunctional inorganic fillers,

* Corresponding authors. Tel.: +61 7 33463828; fax: +61 7 33656074.
E-mail addresses: s.qiao@uq.edu.au (S. Qiao), maxlu@uq.edu.au (G.Q. Lu).

0378-7753/$ – see front matter © 2008 Elsevier B.V. All rights reserved.
doi:10.1016/j.jpowsour.2008.08.094

being both hydrophilic and proton conductive, have also been incorporated into PFSA membranes to give further enhancement of proton conductivity. Among them, solid acid proton conductors such as zirconium phosphate and heteropolyacids have been extensively studied [17–19].

Recently, mesoporous metal oxides have drawn great attention for potential applications as intermediate temperature proton conductors due to their high thermal stability and the superior water adsorption properties of mesopores [20–22]. Furthermore, the mesostructure with a high surface area provides a significant amount of active sites for additional acid functionalization by incorporating protogenic groups to improve the proton conductivity. In the meantime, some attempts have been made to use mesoporous particles as inorganic fillers to modify PFSA membranes [23–25], where improved intermediate temperature proton conductivity and reduced methanol crossover have been obtained compared with the pristine PFSA membrane. On the other hand, most of these fillers generally have a large particle size and irregular morphology, which results in the agglomeration of fillers in the composite membrane [23]. Sambandam and Ramani [26] reported that the properties of composite membranes were greatly influenced by the distribution of fillers in polymer membranes, and that the higher surface-to-volume ratio of fillers as a result of a smaller agglomerate size was more favourable in the property enhancement.

This paper reports the preparation of novel Nafion composite membranes with specifically designed mesoporous MCM-41 silica nanospheres as inorganic fillers. Nanosized and monodisperse spherical particles are expected to provide a homogenous distribution of fillers in the polymer matrix, whilst the periodic mesoporous structure can make fillers act as a water reservoir to consign enhanced water retention properties to the composite membranes. The latter feature is attributed to the large pore volume of mesoporous silica and the capillary interaction of uniform and open mesopores with water adsorption. To the best of our knowledge, this is the first attempt to develop organic–inorganic composite PEMs using such silica fillers. The structures and properties of the prepared Nafion composite membranes with different amounts of silica fillers are examined and discussed. In addition, these prepared membranes are tested in a single DMFC to evaluate their cell performance and methanol crossover in comparison with a pristine Nafion cast membrane.

2. Experimental

2.1. Synthesis of MCM-41 silica fillers

The synthesis of mesoporous MCM-41 silica fillers followed a similar process to that reported by Cai et al. [27]. Typically, 2.1 mL of sodium hydroxide aqueous solution (2 M) was mixed with 288 mL of distilled water. Then, 0.6 g of cetyltrimethylammonium bromide was added to the solution and heated at 80 °C for 30 min. To this clear solution, 3 mL of tetraethoxysilane was added dropwise within 1 min with vigorous stirring. The reaction mixture was then stirred at 80 °C for 2 h. The resultant product was filtered, washed with distilled water and dried at ambient temperature. Finally, the dried sample was calcined in air at 550 °C for 4 h to remove the surfactant.

2.2. Preparation of composite membranes

Composite membranes were prepared by means of a solution casting method. Commercial Nafion solution (15 wt.% in alcohol) was evaporated at 50 °C in an oven for about one week. The obtained Nafion resin was redissolved in dimethyl formamide (DMF) to give a concentration of 20 wt.%. A desired amount of calcined silica fillers was added to the Nafion-in-DMF solution and well-dispersed by ultrasonic treatment. The prepared mixture was poured into a glass Petri dish and then placed on a levelled plate in a 60 °C oven for 24 h. Finally, the solvent in the composite membrane was completely removed at 120 °C in vacuo for 3 h. The membrane was peeled from the Petri dish by immersion in distilled water. The content of silica fillers in the composite membrane was varied to be 1 and 3 wt.%. The membranes were post-treated by boiling in H_2O_2 (3 wt.%) for 1 h, then in H_2SO_4 (1 M) for 90 min, and finally in distilled water for 1 h. Washing with distilled water was repeated several times until the washing solution became neutral. A Nafion cast membrane without silica fillers was prepared via the same procedures for comparison. The composite membranes with 1 and 3 wt.% silica fillers are denoted as Composite-1 and Composite-3, respectively. The three types of membranes were prepared to have approximately in the same thickness of 120–130 μm.

2.3. Characterization

The X-ray diffraction (XRD) pattern of silica fillers was collected on a Rigaku Miniflex X-ray diffractometer with Co Kα ($\lambda = 0.179021$ nm) radiation. The nitrogen sorption isotherm was obtained on a Quantachrome Instruments Quadrasorb SI at 77 K. The specific surface area of silica fillers was calculated using the multiple-point Brunauer–Emmett–Teller (BET) method. The pore-size distribution was determined from the adsorption branch using the Barrett–Joyner–Halenda (BJH) method. Transmission electron microscopy (TEM) was performed using a Tecnai F20 at an acceleration voltage of 200 kV. Scanning electron microscopy (SEM) images were obtained on a JEOL FE 6400. To observe the membrane cross-section, SEM samples were prepared either by cutting the membrane with a blade or by brittle breakage using liquid nitrogen to obtain the smooth fracture surface. Tensile tests were carried out using an Instron model 5543 universal testing machine at a strain rate of 50 mm min^{-1} under ambient conditions. At least three measurements were conducted for each membrane, and the average values were calculated for the determination of the tensile strength and the elongation of tested membranes. Differential scanning calorimetry (DSC) was performed on the hydrated membranes which were equilibrated in water before the DSC testing at a heating rate of 10 °C min^{-1} using a TA Instruments 2920 Modulated DSC. Water uptake was measured by initially drying a membrane in a vacuum oven at 80 °C for 4 h. The dried membrane was weighed, and then immersed in distilled water at ambient temperature for 24 h and re-weighed. Water uptake (wt.%) was calculated from $(W_1 - W_0)/W_0 \times 100\%$, where W_0 and W_1 are the weights of the dried membrane and the hydrated membrane (g), respectively.

The proton conductivity of the membranes was measured by a four-probe method using a Solartron 1260 impedance analyzer. A strip of membrane was placed in a four-probe Teflon cell (BekkTech, USA) that consisted of two outer Pt foils for current application and two inner Pt wires for voltage measurement. By applying a constant a.c. current (10 μA) with frequency ranging from 1 MHz to 1 Hz, the resistance of the membrane was obtained by measuring the voltage drop across two inner Pt wires. The conductivity of the membrane (σ, S cm^{-1}) was defined as $\sigma = L/(A \times R)$, where L is the distance between the two inner Pt wires (cm), A is the cross-sectional area of the membrane (cm^2) and R is the tested membrane resistance (Ω). The temperature and relative humidity (RH) were controlled by a BT-550 gas delivery system (BekkTech, USA).

For single-cell performance tests of a DMFC, the Nafion cast membrane or the composite membrane was made into a membrane–electrode assembly (MEA) with the commercial E-TEK electrodes that consist of gas-diffusion and catalyst layers. The cat-

alyst loadings of Pt–Ru (1:1 a/o) alloy black at the anode and Pt black at the cathode were both 5.0 mg cm^{-2}. The MEA was made by hot pressing at 125 °C for 1 min without pressure and 2 min under 100 kg cm^{-2}. The MEA was assembled in a 5 cm^2 single cell (ElectroChem) and tightened with 2 Nm of torque. The cell test was performed at ambient temperature with the methanol solution (2 M) fed into the anode at the flow rate of 12.4 mL min^{-1} and air passed into the cathode at 75.0 mL min^{-1}. A Solartron 1480 Multistat was used as electric loading to control the fuel cell. In addition, the methanol crossover was tested by the limiting current method [28]. In the testing procedure, the methanol solution passed through the anode and the cathode was purged with nitrogen. The methanol that diffused through the membrane from the anode was catalyzed at the cathode and the generated protons diffused back to the anode. Hence, the reverse current arose only from oxidation of permeated methanol.

3. Results and discussion

3.1. Characterization of silica fillers

Fig. 1a shows the XRD pattern of the calcined silica fillers. Four diffraction peaks can be indexed as (1 0 0), (1 1 0), (2 0 0) and (2 1 0) of a highly ordered two-dimensional hexagonal MCM-41 structure based on the *d* value of each peak (given in the inset of Fig. 1a). The TEM image (Fig. 1b) displays the existence of cylindrical channels and hexagonally arranged pores viewed along different directions of the particles, typically for the highly ordered MCM-41 mesoporous structure. Furthermore, TEM and SEM (Fig. 1c) observations clearly show that the prepared silica fillers are monodisperse spherical nanoparticles with a particle size of ca. 70–140 nm. The nitrogen sorption isotherm (Fig. 1d) of the calcined silica fillers can be classified as a type IV isotherm with a small hysteresis. A steep increase in nitrogen uptake due to capillary condensation inside mesopores occurs at a relative partial pressure of $0.23 < P/P_o < 0.33$, whilst an evident nitrogen adsorption above $P/P_o = 0.9$ should be caused by the interstices among the nanospheres. The prepared fillers exhibit a high BET surface area of 970 m^2 g^{-1}, and a large pore volume of 0.78 cm^3 g^{-1}. The BJH pore-size distribution plot (inset of Fig. 1d) shows a sharp peak at 2.54 nm,which indicates the presence of uniform mesopores. Therefore, mesoporous MCM-41 silica nanospheres have been successfully prepared for use as inorganic fillers in the preparation of the composite membranes.

3.2. Characterization of composite membranes

Fig. 2 presents SEM images of the cross-section of the composite membranes. Generally speaking, silica nanospheres are homogenously embedded in the Nafion matrix for both composite membranes. However, for Composite-1 containing a less amount of fillers, a more homogenous dispersion of fillers can be observed with individual nanospheres nearly in the monodispersed state, as shown in Fig. 2a and b. The composite-3 shows some agglomerates of silica nanospheres (Fig. 2c and d), which suggests that the large amount of incorporation of silica fillers to some extent leads to their agglomeration. The defects observed in the composite membranes (Fig. 2a and c) could be caused by the cutting damage on polymer, as the dense and smooth cross-sectional surface can be seen in the membrane samples prepared by brittle breakage (Fig. 2b and d). In addition, the surface of the composite membranes shows the similar morphology as presented in Fig. 2b and d.

Tensile tests were carried out on the Nafion cast membrane and the composite membranes in order to evaluate their mechanical properties. Fig. 3 gives example tensile curves of the stress–strain response for each membrane. The average values of the tensile strength and the elongation at break (i.e., maximum strain) are listed in Table 1. The tensile strength of the Nafion cast membrane is 15.9 MPa, in fairly good agreement with the reported value of 15.5 MPa in [29], whilst the composite membranes have slightly lower values, namely, 14.0–14.6 MPa. In comparison with that of the

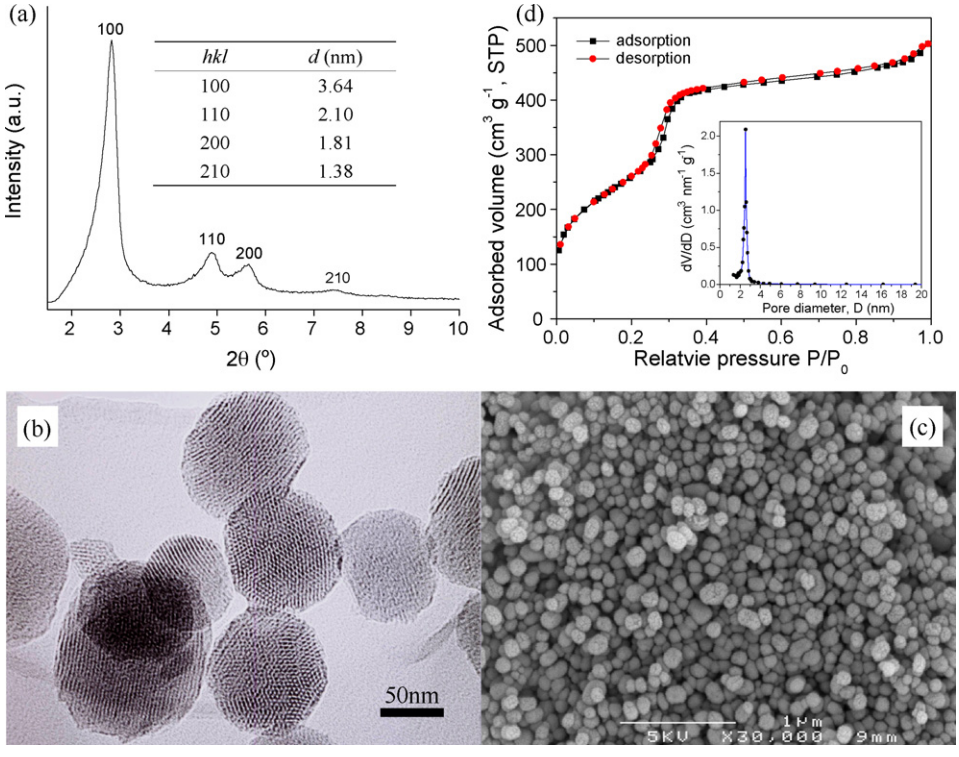

Fig. 1. (a) XRD pattern, (b) TEM, (c) SEM images and (d) nitrogen sorption isotherm of calcined silica fillers. The BJH pore-size distribution is shown in the inset of (d).

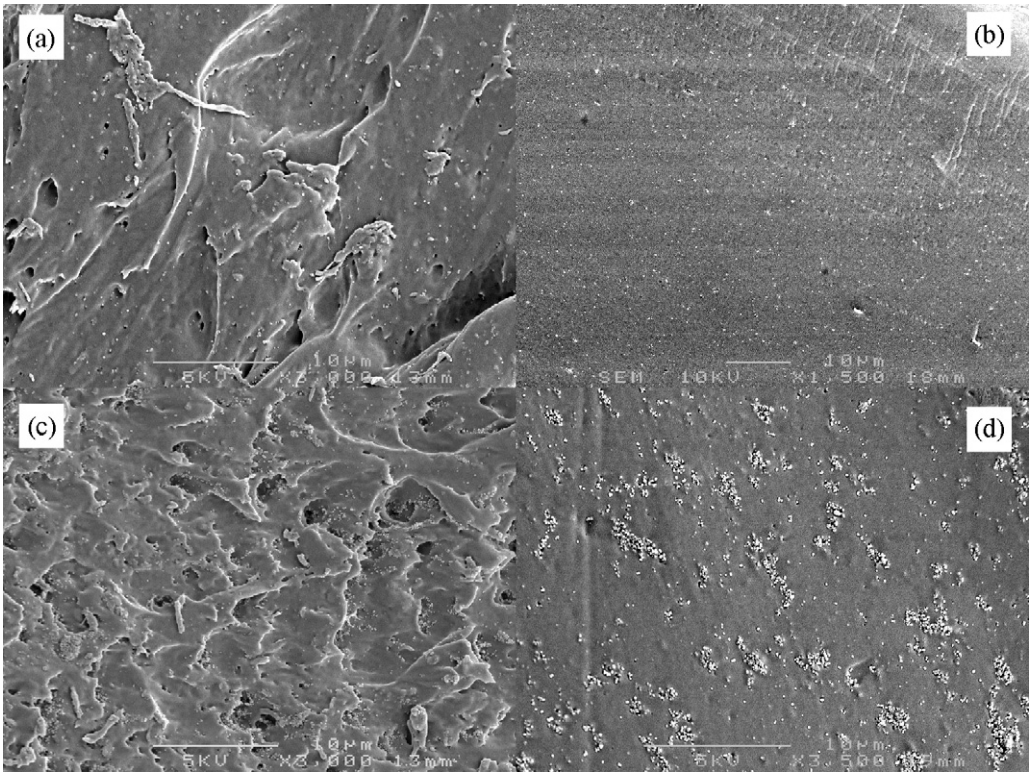

Fig. 2. SEM images of membrane cross-section of Composite-1 (a and b) and Composite-3 (c and d). SEM samples in (a) and (c) were cut by a blade, whilst samples in (b) and (d) were prepared by brittle breakage using liquid nitrogen.

Table 1
Mechanical properties and water uptake of Nafion cast membrane and composite membranes, and the performance of these membranes in DMFC tests

Sample	Tensile strength (MPa)	Elongation at break (%)	Water uptake (wt.%)	Open circuit voltage (V)	Maximum power density ($mW\,cm^{-2}$)	Current density at 0.2 V ($mA\,cm^{-2}$)	Methanol crossover limiting current ($mA\,cm^{-2}$)
Nafion cast	15.9	156.4	19.8	0.49	18.4	90	213
Composite-1	14.0	98.7	24.2	0.57	21.8	108	94
Composite-3	14.6	78.9	30.2	0.53	14.7	72	171

Nafion cast membrane, the elongation of the composite membranes markedly decreases with increasing the filler content, showing a reduction of about 58 and 78% for Composite-1 and Composite-3, respectively. As reported previously [30], the tensile strength of Nafion/mordenite membranes decreases with the content of mordenite, which is likely related to an increase of pores in the membrane due to the decrease of compatibility with surface energy difference between mordenite particle and polymer. Similarly, in the present study, the incorporation of silica nanospheres is not supposed to improve the mechanical strength of pristine Nafion. On the other hand, the smaller elongation for the composite membranes indicates the confinement of fillers on the deformation of pristine Nafion, which can be an advantage by limiting the excessive swelling of the Nafion membrane during fuel cell operation. As a matter of fact, the composite membranes prepared herein have sufficient mechanical properties, including strength and ductility, for fabricating MEAs and performing fuel cell tests. Further SEM observations on the composite membranes after use in DMFC tests were conducted, and no obvious morphological changes of the membranes were detected in micrographs very similar to those in Fig. 2. This suggests that the composite membranes have good structural stability for fuel cell applications.

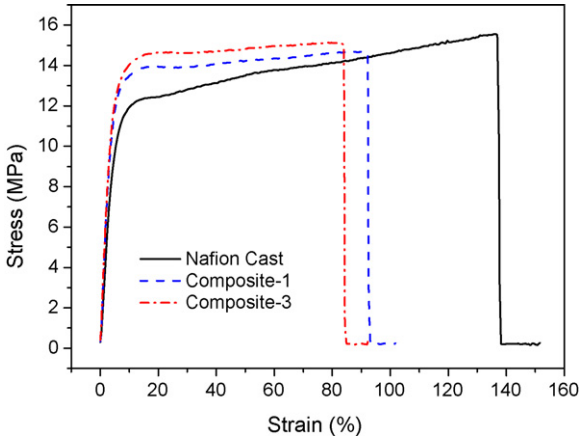

Fig. 3. Example tensile curves of the stress–strain response for Nafion cast membrane and composite membranes.

Water evolution in the Nafion cast membrane, the composite membranes and silica fillers are shown in Fig. 4. The endothermic peaks below 200 °C are indicative of water evaporation. The peak area and the peak temperature position are related to the water content and the affinity of water molecules to the given sample. It can be seen that the composite membranes show an increased amount of water according to the peak area, particularly for Composite-3, which exhibits more than double the peak area of pristine Nafion.

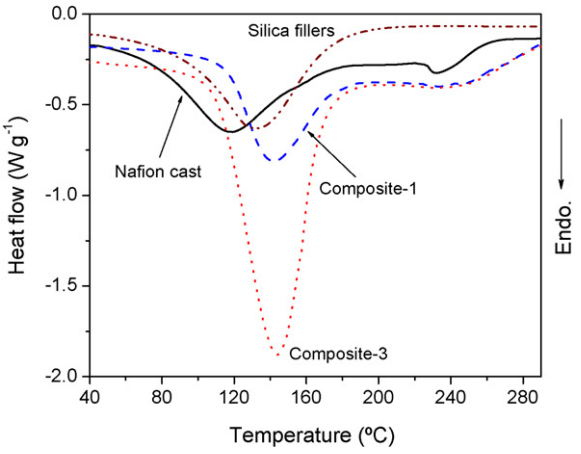

Fig. 4. DSC curves of Nafion cast membrane, composite membranes and silica fillers.

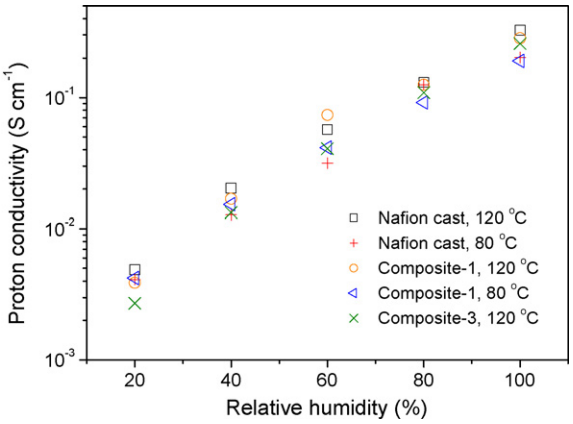

Fig. 5. Proton conductivity of Nafion cast membrane and composite membranes as a function of RH at 80 °C and 120 °C.

This is obviously attributed to the adsorption of water in mesoporous silica fillers. The increased water-storage capacities can be confirmed by water uptake measurements of the membranes, where water uptake (Table 1) of Composite-1 and Composite-3 is increased by 4.4 and 10.4 wt.%, respectively, as compared with 19.8 wt.% for pristine Nafion. On the other hand, the endothermic peaks of both composite membranes become narrow and shift to a temperature of 141–144 °C, much higher than that of the Nafion cast membrane (118 °C). Interestingly, the evaporation peak temperature of the composite membranes is also higher than that of silica fillers (130 °C). The observations suggest that not only the capillary force of mesopores but also the interaction between silica fillers and ionic clusters of the Nafion matrix probably cause the composite membranes to have an enhanced affinity for water molecules. Thus, the enhancement of the water-storage capacities and water-holding strength due to the incorporation of mesoporous fillers is supposed to favour proton transport of Nafion especially at intermediate temperatures and under low humidity conditions. In addition, another peak in the Nafion cast membrane (220–270 °C) can be assigned to the melting of crystalline regions [31], whereas no obvious peaks are detected in the composite membranes. This is a clear indication of the improved thermal stability of the composite membranes due to the addition of inorganic fillers.

To examine the effects of incorporated MCM-41 nanospheres on the proton conductivity at elevated temperatures, the conductivity of the Nafion cast membrane and the composite membranes was measured at 80 and 120 °C and under various humidity conditions.

As shown in Fig. 5, the composite membranes exhibit generally lower proton conductivity than pristine Nafion, and the reduction of conductivity becomes more significant when more silica fillers are incorporated. At 120 °C, Composite-1 shows the conductivity under various RH that is only 10–15% lower than that of Nafion, whereas a 20–40% decrease is observed for Composite-3. In measurements at 80 °C, the conductivity of Composite-1 is very close to Nafion. The conductivity decline is caused by the addition of silica fillers, which are much less conductive than Nafion. However, on a positive note, the addition of fillers only causes a slight decrease in the conductivity, particularly for Composite-1. This is probably related to the homogenous distribution of fillers and the favourable effects of the mesostructure of fillers on water retention and subsequently on proton conduction. Surprisingly, the conductivity of Nafion measured here continuously increases as the temperature increases from 80 to 120 °C and no conductivity decay is detected, which has been observed for the pristine Nafion membrane above 80–90 °C [19,21]. This contradiction could be explained by the results given in a recently published paper [32]. The study reported that the conductivity decays only when the membrane is forced to swell anisotropically along the plane parallel to the membrane surface under the two-probe normal conductivity measurement, whereas no decay is observed even up to 130 °C for the tangential conductivity measured by the four-probe technique that is used in our experiments. Nevertheless, Nafion is still incapable of working at intermediate temperatures above 100 °C because of its limit of glass transition temperature resulting in a reduced dimensional stability of the membrane particularly under highly hydrated conditions, which are necessary to maintain fast proton conductivity [33]. Further, in practical applications, the membrane is assembled into a MEA and constrained normally under a given force, so that the conductivity of Nafion will unavoidably decay.

3.3. DMFC tests

Fig. 6 depicts the DMFC cell performance of three MEAs containing the Nafion cast membrane, Composite-1 or Composite-3. The open circuit voltage (OCV), the maximum power density and the current density at 0.2 V of each membrane are listed in Table 1. Both composite membranes show higher OCVs than pristine Nafion, which implies that the incorporation of fillers reduces the methanol crossover of Nafion. The MEA assembled with Composite-1 presents the best cell performance, with a maximum power density of 21.8 mW cm^{-2}, i.e., ~20% higher than that of pristine Nafion (18.4 mW cm^{-2}). Compared with pristine Nafion, the current density at 0.2 V of Composite-1 is increased by 18 mA cm^{-2} and reaches 108 mA cm^{-2}. By contrast, the per-

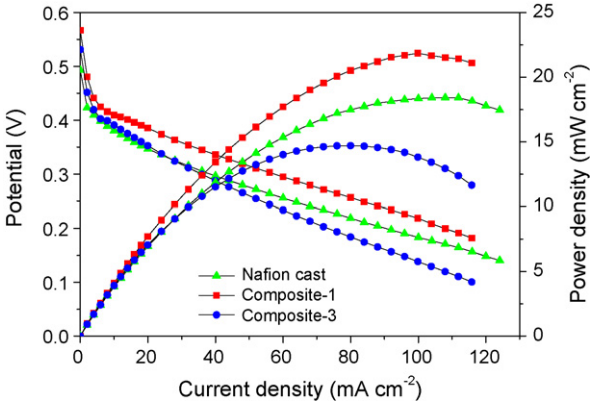

Fig. 6. Polarization curves of DMFC tests with Nafion cast membrane or composite membranes at 20 °C.

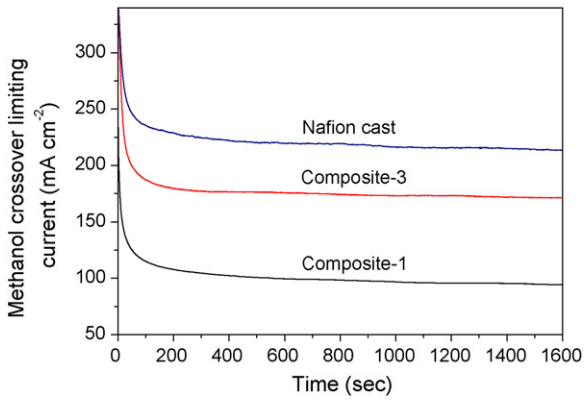

Fig. 7. Methanol crossover limiting current analysis of Nafion cast membrane and composite membranes.

formance of Composite-3 is worse than that of the Nafion cast membrane, even though Composite-3 outperforms Nafion below 25 mA cm^{-2}. Indeed, the performance improvement of the composite membranes at low current densities should arise from the increase of OCV, as reported in literature [34]. The better performance at current densities higher than 25 mA cm^{-2} for the Nafion cast membrane is attributed to its slower voltage drop in the phase of ohmic polarization as a result of its higher proton conductivity. Furthermore, the polarization curves show that the best performance given by Composite-1 is due to its largely increased OCV and similar proton conductivity to pristine Nafion.

The methanol crossover of the membranes was further investigated by applying the limiting current method. As shown in Fig. 7 and Table 1, the incorporation of silica fillers generally suppresses methanol permeation, displaying a lower crossover current in the composite membranes than in the Nafion cast membrane, e.g., about 1.2 times lower in Compoiste-1. Here, Composite-1 shows a more significant reduction in the crossover current than Compoiste-3. This suggests that the addition of fillers does not proportionally reduce the methanol crossover, but ever increases the methanol crossover beyond a certain loading point. The reason for this is probably due to the agglomeration of silica fillers when a high amount is incorporated, as shown by SEM images in Fig. 2c and d. Indeed, the function of fillers is to reduce methanol permeation through restricting the swelling of polymer membranes and blocking the passage of methanol. Agglomerated fillers are less effective than well-dispersed ones, whilst the interstices of nanospheres in agglomerates could facilitate the passage of methanol.

4. Conclusions

Nafion composite membranes have been synthesized for the first time by incorporating mesoporous MCM-41 silica nanospheres. This has been demonstrated to be a valid approach to preparing organic–inorganic composite membranes with a homogenous distribution of inorganic fillers. The incorporation of mesoporous silica nanospheres enhances water retention properties, improves thermal stability, and reduces methanol crossover of pristine Nafion. The composite membranes exhibit slightly lower tensile strength and markedly poorer deformability than the Nafion cast membrane. The proton conductivity of the composite membranes decreases with the increase in the amount of fillers, but only a slight conductivity reduction of about 10–40% is observed in comparison with pristine Nafion. The methanol crossover of the composite membranes is not proportionally decreased with increasing the amount of fillers. This is probably due to the agglomeration of silica nanospheres when a large amount of fillers are incorporated. Composite-1 containing 1 wt.% of fillers displays a higher OCV and a better DMFC performance than the Nafion cast membrane. This is attributed to the similar conductivity of Composite-1 to pristine Nafion, and its markedly reduced methanol crossover, i.e., ~1.2 times lower, as verified by limiting current analysis.

Acknowledgements

The authors acknowledge financial support for this work from the Australian Research Council and an ARC Federation Fellowship (to Prof. G.Q. Lu).

References

[1] V. Mehta, J.S. Cooper, J. Power Sources 114 (2003) 32–53.
[2] X.G. Li, Principles of Fuel Cells, Taylor & Francis Group, New York, 2006, pp. 1–19.
[3] J.H. Wee, Renew. Sust. Energ. Rev. 11 (2007) 1720–1738.
[4] F. Barbir, PEM Fuel Cells: Theory and Practice, Elsevier Ltd., Amsterdam, 2005.
[5] F.A. de Bruijn, R.C. Makkus, R.K.A.M. Mallant, G.J.M. Janssen, in: T.S. Zhao, K.-D. Kreuer, T.V. Nguyen (Eds.), Advances in Fuel Cells, Elsevier Ltd., Amsterdam, 2005, pp. 248–275.
[6] B. Smitha, S. Sridhar, A.A. Khan, J. Membr. Sci. 259 (2005) 10–26.
[7] K.A. Mauritz, R.B. Moore, Chem. Rev. 104 (2004) 4535–4585.
[8] W.H.J. Hogarth, J.C. Diniz da Costa, G.Q. Lu, J. Power Sources 142 (2005) 223–237.
[9] Q.F. Li, R.H. He, J.O. Jensen, N.J. Bjerrum, Chem. Mater. 15 (2003) 4896–4915.
[10] J.L. Zhang, Z. Xie, J.J. Zhang, Y.H. Tang, C.J. Song, T. Navessin, Z.Q. Shi, D.T. Song, H.J. Wang, D.P. Wilkinson, Z.S. Liu, S. Holdcroft, J. Power Sources 160 (2006) 872–891.
[11] A. Heinzel, V.M. Barragan, J. Power Sources 84 (1999) 70–74.
[12] K.T. Adjemian, S.J. Lee, S. Srinivasan, J. Benziger, A.B. Bocarsly, J. Electrochem. Soc. 149 (2002) A256–A261.
[13] M.L. Di Vona, Z. Ahmed, S. Bellittto, A. Lenci, E. Traversa, S. Licoccia, J. Membr. Sci. 296 (2007) 156–161.
[14] V. Tricoli, F. Nannetti, Electrochim. Acta 48 (2003) 2625–2633.
[15] D.H. Jung, S.Y. Cho, D.H. Peck, D.R. Shin, J.S. Kim, J. Power Sources 118 (2003) 205–211.
[16] V. Neburchilov, J. Martin, H.J. Wang, J.J. Zhang, J. Power Sources 169 (2007) 221–238.
[17] G. Alberti, M. Casciola, D. Capitani, A. Donnadio, R. Narducci, M. Pica, M. Sganappa, Electrochim. Acta 52 (2007) 8125–8132.
[18] H.J. Kim, Y.-G. Shul, H. Han, J. Power Sources 158 (2006) 137–142.
[19] B. Mecheri, A. D'Epifanio, E. Traversa, S. Licoccia, J. Power Sources 169 (2007) 247–252.
[20] R. Marschall, I. Bannat, J. Caro, M. Wark, Microporous Mesoporous Mater. 99 (2007) 190–196.
[21] Y. Daiko, T. Kasuga, M. Nogami, Microporous Mesoporous Mater. 69 (2004) 149–155.
[22] M.I. Ahmad, S.M.J. Zaidi, S. Ahmad, J. Power Sources 157 (2006) 35–44.
[23] Y. Tominaga, I.C. Hong, S. Asai, M. Sumita, J. Power Sources 171 (2007) 530–534.
[24] Y.-F. Lin, C.-Y. Yen, C.-C.M. Ma, S.-H. Liao, C.-H. Lee, Y.-H. Hsiao, H.-P. Lin, J. Power Sources 171 (2007) 388–395.
[25] C.S. Karthikeyan, S.P. Nunes, L.A.S.A. Prado, M.L. Ponce, H. Silva, B. Ruffmann, K. Schulte, J. Membr. Sci. 254 (2005) 139–146.
[26] S. Sambandam, V. Ramani, J. Power Sources 170 (2007) 259–267.
[27] Q. Cai, Z.S. Luo, W.Q. Pang, Y.W. Fan, X.H. Chen, F.Z. Cui, Chem. Mater. 13 (2001) 258–263.
[28] Z. Qi, A. Kaufman, J. Power Sources 110 (2002) 177–185.
[29] D.H. Kang, D. Kim, Korean J. Chem. Eng. 24 (2007) 1101–1105.
[30] S.-H. Kwak, T.-H. Yang, C.-S. Kim, K.H. Yoon, Solid State Ionics 160 (2003) 309–315.
[31] H.R. Corti, F. Nores-Pondal, P.M. Buera, J. Power Sources 161 (2006) 799–805.
[32] M. Casciola, G. Alberti, M. Sganappa, R. Narducci, J. Power Sources 162 (2006) 141–145.
[33] G. Alberti, M. Casciola, L. Massinelli, B. Bauer, J. Membr. Sci. 185 (2001) 73–81.
[34] C.-Y. Yen, C.-H. Lee, Y.-F. Lin, H.-L. Lin, Y.-H. Hsiao, S.-H. Liao, C.-Y. Chuang, C.-C.M. Ma, J. Power Sources 173 (2007) 36–44.